IEEE Access
Multidisciplinary | Rapid Review | Open Access Journal

Received June 8, 2021, accepted July 2, 2021, date of publication July 19, 2021, date of current version July 29, 2021.

Digital Object Identifier 10.1109/ACCESS.2021.3098316

Reconstructing Underwater Temperature Spatial Distribution Using Ultrasound Tomography

XIAOJIAN YU[1], SONG LIN[2], XIONGYE HONG[3,4], AND HONGHUI HUANG[5]

[1]School of Biological Science and Biotechnology, Minnan Normal University, Zhangzhou, Fujian 363000, China
[2]College of Ocean and Earth Science, Xiamen University, Xiamen, Fujian 361100, China
[3]Fujian Coastal Sea Environmental Monitoring Station, Putian, Fujian 351100, China
[4]Guangdong Provincial Key Laboratory of Fishery Ecology and Environment, South China Sea Fisheries Research Institute, Chinese Academy of Fishery Sciences, Guangzhou 510300, China
[5]Southern Marine Science and Engineering Guangdong Laboratory (Guangzhou), Guangzhou 511485, China

Corresponding author: Xiaojian Yu (jen_yu@163.com)

This work was supported in part by the Natural Science Foundation of Fujian Province of China under Grant 2020J01808; in part by the National Natural Science Foundation of China under Grant 11874311, Grant 41676023, Grant 41276040, and Grant 41422604; in part by the University-Industry Cooperation Project in Fujian Province under Grant 2018Y4012; in part by the Special Fund for Marine and Fishery Development of Xiamen under Grant 20CZB015HJ01; and in part by the Water Conservancy Science and Technology Innovation Project of Guangdong under Grant 2020-16.

ABSTRACT Temperature has a great impact on underwater environment. In this study, a grid-based scheme of underwater ultrasound tomography was proposed to reconstruct temperature spatial distribution. Computer simulations showed that ultrasound tomography reconstructed the distributed temperature pattern of Daya Bay seawater. The water pool experiment showed that the reconstructed temperature was consistent with in situ temperature. The ultrasound tomography had advantages in reducing measurements to extract the temperature spatial pattern over the in-situ method, and in increasing measurement accuracy over low frequency acoustic scheme. The results suggest that underwater ultrasound tomography may provide a valuable approach to reconstruct high spatial resolution temperature distribution at small-scale coastal, estuary, and sea-land interface regions.

INDEX TERMS Ultrasound tomography, underwater temperature, small-scale coastal regions.

I. INTRODUCTION

Underwater acoustic technique plays a significant role in marine scientific research and ocean engineering [1], [2]. Unlike the limited transmission distance of optical and electromagnetic waves in sea waters due to high attenuation, acoustic waves may propagate across oceans for thousands of kilometers [3]. In large-scale and meso-scale regions, low frequency acoustic tomography has been widely studied since late 1970s [4]. Acoustic tomography of ocean climate project was proposed to monitor global ocean temperature [5]. Low frequency acoustic transmission was conducted to obtain temperature variation of arctic ocean water [6] and to monitor heat content across the Mediterranean Sea [7]. Low central frequencies such as 40 Hz, 100-to 200-Hz, and 400 Hz lead to low temporal as well as spatial resolutions of acoustic tomography. However, for small-scale (<10 kilometer) coastal, estuary, and sea-land interface regions, low frequency acoustic tomography might not be applicable [8]–[12]. Small-scale coastal, estuary, and sea-land interface regions are located at the junction of ocean and land. The tortuous coastline, combined with surface runoff, ocean tide, and wind, leads to the complex and highly variable distribution of shallow water temperature. To understand physical process of the underwater ecosystems in these small regions, high spatial resolution reconstruction of fine temperature distribution is very important. In-situ sensors such as water thermometer and conductivity-temperature-depth profiler (CTD) have been commonly used [13], [14]. However, to obtain fine temperature spatial distribution, these in-situ measurements lead to significant increases in time and cost. In addition, these in-situ sensors have the risk of being destroyed under extreme weather conditions, such as typhoon and flooding. Our recent study has shown that high frequency acoustic technique provides real-time observation of range-averaged flow velocity, however, its application in reconstructing fine spatial distribution has not been found [8]. Therefore, there is an urgent demand for developing high spatial resolution

The associate editor coordinating the review of this manuscript and approving it for publication was Jiajia Jiang.

acoustic tomography for small-scale (<10 kilometer) coastal, estuary, and sea-land interface regions.

Ultrasound tomography is a novel imaging technology used to reconstruct a map of sound speed in a medium based upon the arrival times of ultrasound waves transmitted from various directions. It provides an effective way to overcome the low resolution limitation of low frequency acoustic techniques. Ultrasound tomography has received wide interest in medical imaging, ultrasonic inspection, seismic imaging, etc. [15]–[19]

In this study, underwater ultrasound tomography (UUT) will be proposed to reconstruct high spatial resolution distribution of underwater temperature. Based on the reciprocal transmission principle, a grid-based UUT algorithm is derived. Furthermore, the grid-based UUT technique is applied to reconstruct fine temperature distribution of the seawater in the Daya Bay. Finally, a water pool experiment with ultrasound frequency of 60 kHz is performed to verify the temperature reconstruction principle. The temperature reconstructed by UUT is compared with the measured temperature by CTD.

II. MATERIALS AND METHODS

For high frequency UUT, a ray model could be used to describe ultrasound transmission [17], [18]. Consider a two-dimensional observation area, an ultrasound station A is positioned, and the other station B moves around A for measurement, as shown in Fig. 1(a). For the square region of the grid-based UUT, station B has N-time measurement at each side, giving the measurement number of N. Thus, for four sides, station B has $4N-4$ measurement number. Clearly, for in-situ measurements, such as CTD or water thermometer, N^2 measurement number is required to obtain the whole two-dimensional temperature distribution.

Based on the reciprocal transmission principle [8]–[12], [14], ray propagation time between A and B would be affected by the sound speed distribution c(x,y) and current $\mathbf{u}\,(x, y)$.

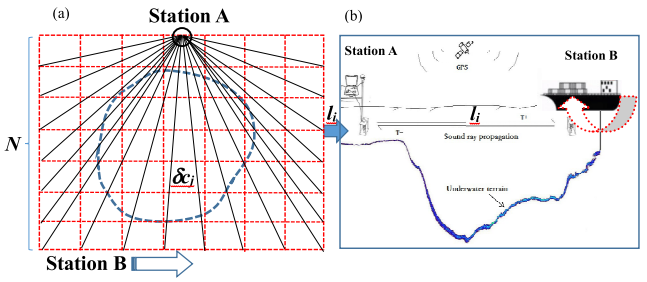

FIGURE 1. (a) Illustration of the grid-based UUT scheme; (b) Reciprocal ultrasound transmission of two ultrasound stations. For more details, see text.

We proposed a grid-based UUT scheme to reconstruct the sound speed distribution as $c(x, y) = c_0 + \delta c(x, y)$. c_0 is the reference sound speed and $\delta c(x, y)$ is the sound speed variation of the studied region. N positions are placed along each side of the area, leading to $N \times N$ matrix of $\delta c(x, y)$ and m direct rays between A and B. Clearly, N gives the grid number. The reciprocal propagation times of the i-th ray l_i between A and B can be described as [8], [20]:

$$T_i^+ = \int_{l_i} \frac{\mathrm{ds}}{c_0 + \delta c + \mathbf{u} \bullet \mathbf{n}} \tag{1}$$

and

$$T_i^- = \int_{l_i} \frac{\mathrm{ds}}{c_0 + \delta c - \mathbf{u} \bullet \mathbf{n}} \tag{2}$$

T_i^+ is the transmission time from station A to B and T_i^- is the transmission time from station B to A, as shown in Fig. 1(b). $\mathbf{n}$ is the normal vector of ultrasound rays. Let T_{i0} be the reference propagation time of the i-th ray l_i at the reference sound speed c_0. For sufficiently small time differences $\delta T_i^+ = T_i^+ - T_{i0} \ll T_i^+$ and $\delta T_i^- = T_i^- - T_{i0} \ll T_i^-$, under the first-order approximation, Eqs. (1) and (2) can be obtained as

$$T_i^+ \approx T_{i0} - \int_{l_i} \frac{\delta c \mathrm{ds}}{c_0^2} - \int_{l_i} \frac{\mathbf{u} \bullet \mathbf{n} \mathrm{ds}}{c_0^2} \tag{3}$$

and

$$T_i^- \approx T_{i0} - \int_{l_i} \frac{\delta c \mathrm{ds}}{c_0^2} + \int_{l_i} \frac{\mathbf{u} \bullet \mathbf{n} \mathrm{ds}}{c_0^2} \tag{4}$$

Clearly, sound speed variation satisfies:

$$\frac{\delta T_i^+ + \delta T_i^-}{2} \approx -\int_{l_i} \frac{\delta c \mathrm{ds}}{c_0^2} \tag{5}$$

Let sound speed variation in the j-th grid is δc_j, and then the corresponding ray length within the j-th grid of l_i is l_{ij}. For the sufficiently large grid number N in small-scale regions, we consider $l_{ij}/c_0^2 \rightarrow \mathrm{ds}$ and then Eq.(5) can be approximated as

$$\frac{\delta T_i^+ + \delta T_i^-}{2} \approx \sum_{j=1}^{m} \frac{-l_{ij}}{c_0^2} \delta c_j \tag{6}$$

Eq. (6) can be described in the matrix form as,

$$\mathbf{y} = \mathbf{E}\mathbf{x} + \mathbf{e} \tag{7}$$

where y is the measurement result satisfying $y_i = \frac{\delta T_i^+ + \delta T_i^-}{2}$, $\mathbf{E}$ is the known transfer coefficients matrix satisfying $E_{ij} = -\frac{l_{ij}}{c_0^2}$, $\mathbf{x}$ is the reconstructed vector satisfying $x_j = \delta c_j$, and $\mathbf{e}$ is the error vector. From the determined δT_i^+, δT_i^-, and $\frac{-l_{ij}}{c_0^2}$, the sound speed variation δc_j can be reconstructed by solving Eq. (7). We then use the least square method

$$\mathbf{x} \approx (\mathbf{E}^{\mathrm{T}}\mathbf{E})^{-1}\mathbf{E}^{\mathrm{T}}\mathbf{y} \tag{8}$$

In the grid-based UUT method, the ray number usually is much larger each grid of sound speed variation. The inverse problem of Eq. (7) is a well-posed one by using the least square method. In the surrounding region in Fig. 1(a), the ray number may equal to the grid number, and thus the error $\mathbf{e}$ may affect the reconstruction quality. However, in the center region, the ray number is much larger than the grid number,

and thus the reconstruction error would be reduced. Thus the sound speed distribution c(x,y) = c0+δc(x,y) can be reconstructed by using the grid-based UUT scheme.

Furthermore, the sound speed can be transformed into temperature based on the Del Grosso equation [19] as:

$$c = c_0 + \Delta c_T + \Delta c_P + \Delta c_S + \Delta c_{STP} \tag{9}$$

where T, P and S represent temperature, pressure, and salinity, respectively. c_0, Δc_T, Δc_P, Δc_S, and Δc_{STP} satisfy:

$$\begin{aligned}
c_0 &= 1402.392,\\
\Delta c_T &= 5.01109398873 \cdot T - 0.0550946843172 \cdot T^2\\
&\quad + 0.000221535969240 \cdot T^3,\\
\Delta c_S &= 1.32952290781 \cdot S + 0.000128955756844 \cdot S^2,\\
\Delta c_P &= 0.15605925041 \cdot P + 0.0000244998688441 \cdot P^2\\
&\quad - 0.88392332513 \cdot 10^{-8} \cdot P^3,\\
\Delta c_{STP} &= -0.0127562783426 \cdot T \cdot S\\
&\quad + 0.0063519163389 \cdot T \cdot P\\
&\quad + 0.265484716608 \cdot 10^{-7} \cdot T^2 \cdot P^2\\
&\quad - 0.159349479045 \cdot 10^{-5} \cdot T \cdot P^2\\
&\quad + 0.522116437235 \cdot 10^{-9} \cdot T \cdot P^3\\
&\quad - 0.438031096213 \cdot 10^{-6} \cdot T^3 \cdot P\\
&\quad - 0.161674495909 \cdot 10^{-8} \cdot S^2 \cdot P^2\\
&\quad + 0.968403156410 \cdot 10^{-4} \cdot T^2 \cdot S\\
&\quad + 0.485639620015 \cdot 10^{-5} \cdot T \cdot S^2 \cdot P\\
&\quad - 0.340597039004 \cdot T \cdot S \cdot P.
\end{aligned} \tag{10}$$

For the studied shallow water area, we consider that the salinity and pressure are stable and can be measured by using CTD. From Eqs. (8), (9) and (10), we can reconstruct the two-dimensional shallow water temperature distribution using the grid-based UTT algorithm. By generalizing the two dimension grids to the three dimension grids, the grid-based UUT method may be applied to study the three-dimensional case where temperature varies according to depth.

III. RESULTS AND DISCUSSION

Based on the above grid-based UTT principle, we examined the underwater temperature distribution in Daya Bay. The original temperature data was obtained by the voyage survey of South China Sea Fisheries Research Institute, Chinese Academy of Fishery Sciences in January 2020 in Daya Bay, as shown in Fig. 2(a). CTD (CastAway, YSI, Yellow Springs, OH) with the temperature measurement accuracy ±0.05 °C was used to obtain the underwater temperature distribution of the sea area with a 10 × 10 grid and 0.5-meter depth. The measured salinity was 32.3 ‰. Figure 2(b) shows the increase of temperature at the upper left-hand corner. It suggests that the warm water in Daya Bay might have an impact on coastal environment. The averaged underwater temperature of A1-A8 was 1.8 °C higher than those of A9 and A10, and the water temperature of D3 was the highest. We then applied the grid-based UUT algorithm to calculate the sound

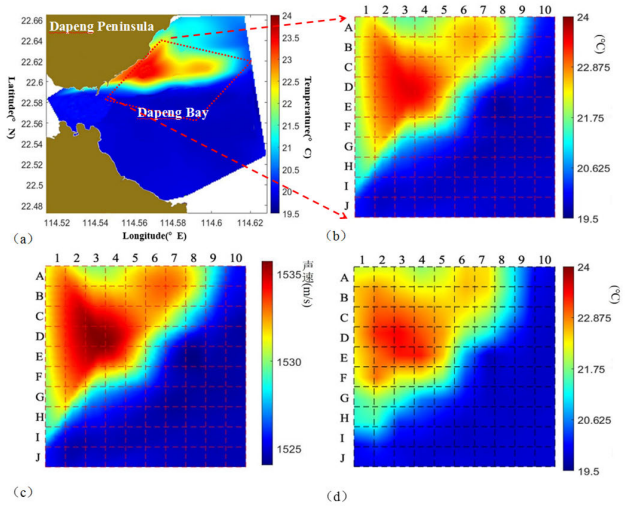

FIGURE 2. (a) CTD measurement in Daya Bay, China; (b) Original temperature distribution near Daya Bay; (c) Sound speed distribution near Daya Bay; (d) Reconstructed temperature distribution by the grid-based UUT method.

propagation time and reconstructed the corresponding underwater temperature. Figure 2(c) gives the sound speed distribution of underwater near Daya Bay. Figure 2(d) shows the reconstructed temperature spatial pattern of UUT, where the grid number is 10. The goodness of fit of the reconstructed and original temperature data is 0.98, suggesting their high correlation relationship. The reconstructed results by UUT show that A1-A9 have higher water temperatures than A10, which is slightly larger than the measured area. It may be associated with the spatial smoothing effect during reconstruction. D3 has the highest temperature, which is the same as the measured area.

Figure 3 compares the measured temperatures by CTD and the reconstructed temperatures by UUT. The mean temperature value and the standard deviation of CTD were 20.42 °C and 0.99 °C, while the mean temperature value and the standard deviation of UUT were 21.02 °C and 1.26 °C. The relative difference between the reconstructed and original temperatures is less than 4.1%, indicating that the reconstructed UUT results are qualitatively consistent with the measured CTD results.

In order to verify UUT, we performed an ultrasound transmission experiment in a large water pool with length × width × height of 27 m × 14.6 m × 4 m. A reciprocal transmission system of UUT was designed, as shown in the block diagram (Fig. 4). Ultrasound transducers with central frequency f_c of 60 kHz and bandwidth of 20 kHz were used. Ultrasound stations A and B both included transmitter and receiver. In the transmitter, the ultrasound signal modulated by sine-wave 63-chip M-sequence was generated every 10-seconds. The signal was then D/A converted by data acquisition card with the sampling rate 400 kHz (NI USB-6216, National Instruments, USA). After power amplification, the underwater ultrasound signal x(t) was transmitted by

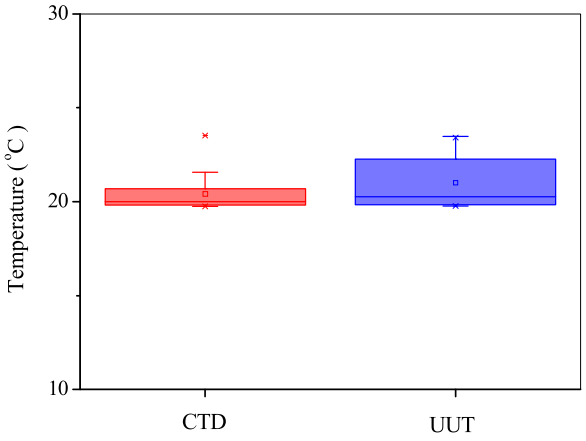

FIGURE 3. Comparison of the measured CTD temperatures and reconstructed UUT temperatures.

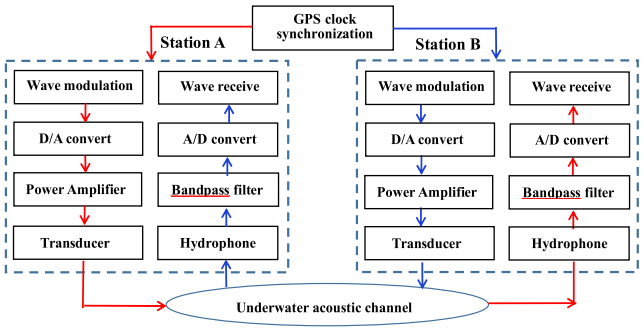

FIGURE 4. Systematic diagram of UUT systems.

the ultrasound transducer with 1.8 m depth. In the receiver, the ultrasound signal y(t) was recorded by the hydrophone (8103, Bruel and Kjeer, Neerum, Denmark) within a frequency range of 0.1 Hz to 180 kHz. An 8th-order Butterworth bandpass filter with the pass-band of 40-80 kHz was used to filter out low frequency noise. After A/D conversion, the signal was sent into computer for further processing. The signal transmission and reception were synchronized with the GPS clock with the time precision of 20 ns. We set the salinity of fresh water. The water temperature near station A was measured by CTD for comparison.

We then performed the underwater ultrasound experiments, as shown in Fig. 5(a). Station A was positioned at the middle point of the pool length. Station B moved around with the distance interval of 1m and the time interval of 10s. Each length side has 25 measurements and each width side has 14 measurements. A total of 78 measurement numbers were taken in a working cycle. Surface and bottom of the shallow water caused the multiple path of ultrasound transmission in Fig. 5(b). Paths 1 and 2 correspond to the direct ray and the surface reflected ray, respectively. The received ultrasound signals at stations B and A are shown in Figs. 5(c) and (d). The received signal amplitudes were much larger than background noises, contributing to the power amplifier and bandpass filter. We performed the cross-correlation analysis for the transmitted and received signals. Peak values of the correlation function gave the arrival times from the transmitter

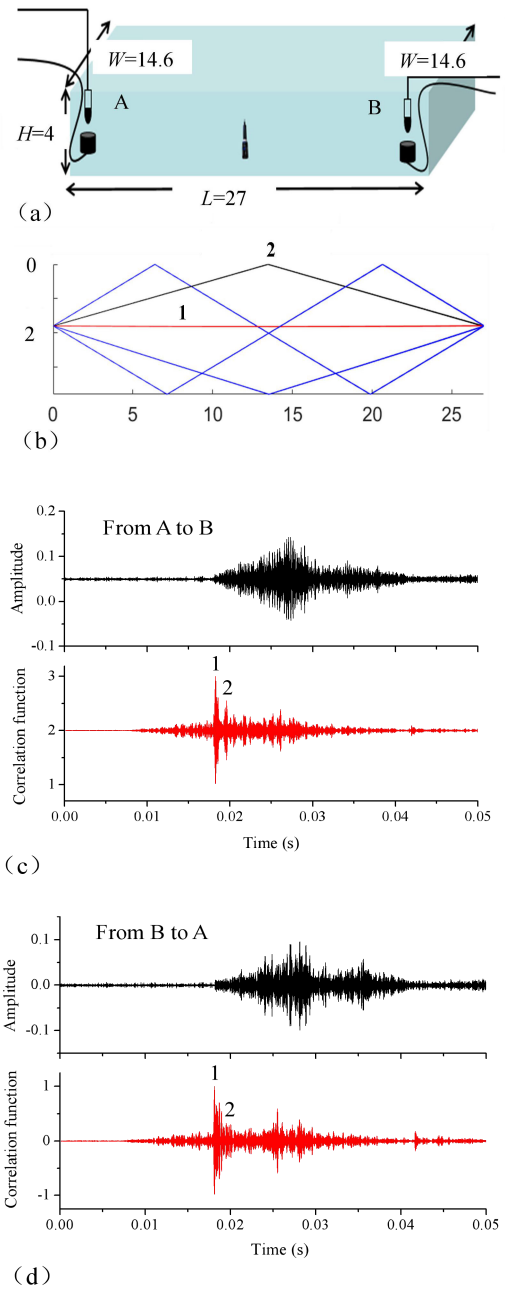

FIGURE 5. (a) Systematic diagram of underwater ultrasound experiments; (a) Multiple acoustic paths, where 1 and 2 denote the direct path and the surface reflected path, respectively; (c)The received signal at station B (upper) and the correlation analysis between the transmitted and received signals (lower), where 1 and 2 denote the direct path and the surface reflected path, respectively; (d)The received signal at station A (upper) and the correlation analysis between the transmitted and received signals (lower).

to receiver. The propagation times and of the ultrasound wave between A and B were estimated about 0.01814 ms, leading to the reconstructed temperature of 19.41°C. For 60 kHz of the transducer frequency, the acoustic period was about 16.7 ms, which was much larger than the time precision 20 ns of GPS. Thus, high resolution GPS in this study significantly

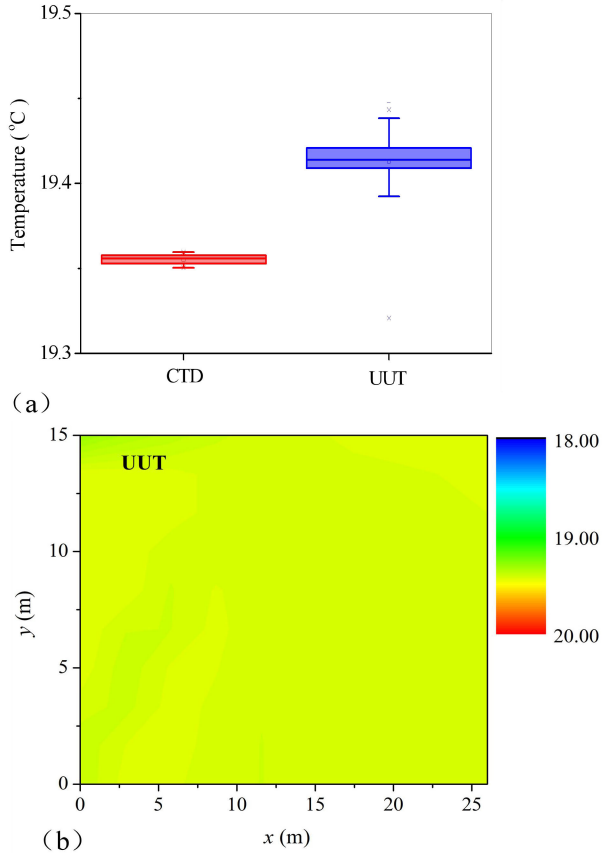

FIGURE 6. (a) Comparison of the measured CTD temperatures and reconstructed UUT temperatures, where 2-hour temperature data were given; (b) Reconstructed underwater temperature distribution by the grid-based UUT method.

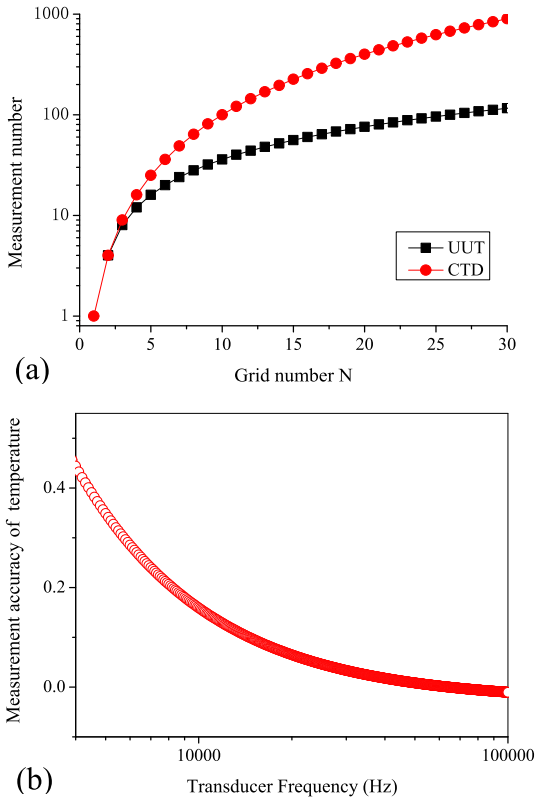

FIGURE 7. (a) Measurement number comparison of CTD and UUT with respect to grid number N; (b) The effect of transducer frequency on the measurement accuracy of the underwater temperature.

reduced the measurement error of propagation time. In addition, UUT has the high temperature reconstruction accuracy. For small-scale Jiulongjiang sea-land interface with $L = 390$ m [8], the reconstruction accuracy of 60 kHz was calculated as 0.002°C, which was much less than 0.05°C of the CastAway CTD applied in this study. The reconstruction accuracy of acoustic tomography with 23.7 kHz was almost the same with that of CTD. However, the reconstruction accuracy 0.349°C of acoustic tomography with 5 kHz would be much lower than CTD, suggesting that lower frequency acoustic tomography might not be applicable for small-scale ocean regions, such as coastal area, bay, estuary, sea-land interface, etc.

Furthermore, we tested the stability of UUT performance, where the transmission time interval was set to 1 minute and the total test time was 2 hours. As shown in Fig. 6(a), the 2-hour averaged temperature of UUT is 19.43 °C. CTD measurement gave the average temperature of 19.35°C, leading to the relative error 0.4%. Furthermore, in comparison with the in-situ CTD measurement, the grid-based UUT scheme allows to reconstruct the spatial distribution of the underwater temperature, as shown in Fig. 6(b), where the grid number of each length was 25, and the grid number of each width was 14. Temperature of the right side of the water pool was slightly higher than that of the left side. Circulating water system in the 27m × 14.6m × 4m water pool might cause the temperature change from 19.30°C to 19.45°C. Clearly, such a small-scale temperature distribution could not be reconstructed by either using low frequency underwater acoustic technique [4]–[7], [9], [14] or high frequency acoustic tomography [8], [11].

In this study, high frequency ray model was applied for small-scale shallow water. For the application of long distance propagation in seawater, refraction effect should be considered to determine the ray path. According to the principle of underwater acoustics [6], for the deep isothermal layer, sound velocity gradient may lead to the ray radius about 89.6 km, which is much large than small-scale (<10 km) coastal, estuary, and sea-land interface regions. In this study, the length of the study region in Daya Bay was about 5 km, and thus the refraction effect may not be significant. For the experiment with distance 0.027km and ultrasound frequency 60 kHz, refraction effect may be negligible. Thus, ray path could to assumed be straight in this study.

Finally, as shown in Fig. 1, the grid-based UUT scheme may require the $4N-4$ computation load to reconstruct the two-dimensional underwater temperature distribution of the study area, however, in-situ CTD or water thermometer require the N^2 computation load to obtain the temperature distribution. As shown in Fig. 7(a), UUT and CTD have the

same measurement number for the grid number $N = 2$. However, for $N = 10$ in Fig. 2, the 36 measurement number of UUT were much less than the 100 measurements of CTD to obtain the temperature distribution in Daya Bay. Increasing grid size N may increase computation load. For significantly larger N, $4N-4$ would be much less than N^2 in Fig. 7(a). Thus, the grid-based UUT method proposed in this study has the obvious advantage in reducing computation load than the in-situ CTD method [13], [14]. In addition, the spatial resolution of the UUT method is proportional to $1/N$. The larger N is, the higher the spatial resolution is. Furthermore, according to Eq.(5), the measurement accuracy of time may increase with transducer frequency. As shown in Fig. 7(b), the measurement accuracy of temperature increases with the transducer frequency. For ultrasound frequency 60 kHz, the measurement accuracy is ± 0.002 °C, while for 10 kHz, the measurement accuracy is ± 0.159 °C. Lower accuracy of low frequency acoustic technique might limit their applications in small spatial scales [4]–[12]. Therefore, UUT may overcome low spatial as well as temporal resolutions of low frequency acoustic tomography. Consider that temperature distribution plays an important role for underwater ecosystems [20], these advantages allow UUT to capture fine environmental characteristic of small-scale coastal, estuary, and sea-land interface regions.

IV. CONCLUSION

In this paper, a grid-based UUT scheme was proposed to reconstruct underwater temperature distribution. Reciprocal acoustic transmission principle of UUT was derived. Computer simulations showed the distributed temperature pattern of Daya Bay seawater. The correlation coefficient between the reconstructed results and original data was 0.98, allowing for the reconstruction of fine spatial distribution of the underwater temperature in Daya Bay area. Furthermore, the feasibility of UUT was examined by a water pool experiment. The reconstructed temperature by UUT showed good agreement with the measured temperature by CTD with the relative error of 0.3%. The grid-based UUT method has an obvious advantage in reducing measurement numbers than the in-situ CTD method. Small-scale coastal, estuary, and sea-land interface regions are the concentrated area of human marine activities. Temperature has a great impact on the biological, chemical, and physical properties of underwater environment. Our study suggests that ultrasound tomography might provide an effective tool to monitor high spatial resolution underwater temperature characteristic of these small-scale ocean regions.

REFERENCES

[1] G. Han, S. Shen, H. Song, T. Yang, and W. Zhang, "A stratification-based data collection scheme in underwater acoustic sensor networks," *IEEE Trans. Veh. Technol.*, vol. 67, no. 11, pp. 10671–10682, Nov. 2018.

[2] J. Jiang, G. Han, C. Zhu, S. Chan, and J. J. P. C. Rodrigues, "A trust cloud model for underwater acoustic sensor networks," *IEEE Commun. Mag.*, vol. 55, no. 3, pp. 110–116, Mar. 2017.

[3] T. Falardeau and P. Belanger, "Ultrasound tomography in bone mimicking phantoms: Simulations and experiments," *J. Acoust. Soc. Amer.*, vol. 144, no. 5, pp. 2937–2946, Nov. 2018.

[4] C. Tao and X. Liu, "Reconstruction of high quality photoacoustic tomography with a limited-view scanning," *Opt. Exp.*, vol. 18, pp. 2760–2766, 2010.

[5] M. Jaeger and M. Frenz, "Towards clinical computed ultrasound tomography in echo-mode: Dynamic range artefact reduction," *Ultrasonics*, vol. 62, pp. 299–304, Sep. 2015.

[6] K. R. Leonard and M. K. Hinders, "Guided wave helical ultrasonic tomography of pipes," *J. Acoust. Soc. Am.*, vol. 144, pp. 2937–2946, Aug. 2018.

[7] E. E. Tudisco, P. Roux, S. A. Hall, G. M. B. Viggiani, and G. Viggiani, "Timelapse ultrasonic tomography for measuring damage localization in geomechanics laboratory tests," *J. Acoust. Soc. Amer.*, vol. 37, p. 1389, 2015.

[8] R. J. Urick, *Principles of Underwater Sound*, 2nd ed. New York, NY, USA: McGraw-Hill, 1975.

[9] W. Munk and C. Wunsch, "Ocean acoustic tomography: A scheme for large scale monitoring," *Deep Sea Res. A, Oceanographic Res. Papers*, vol. 26, no. 2, pp. 123–161, Feb. 1979.

[10] W. H. Munk, "Acoustic thermometry of ocean climate (ATOC)," *J. Acoust. Soc. Amer.*, vol. 97, no. 5, p. 3233, 1995.

[11] P. N. Mikhalevsky, A. B. Baggeroer, A. Gavrilov, and M. Slavinsky, "Continuous wave and M-sequence transmissions across the arctic," *J. Acoust. Soc. Amer.*, vol. 96, no. 5, pp. 3235–3236, Nov. 1994.

[12] U. Send, G. Krahmann, D. Mauuary, Y. Desaubies, F. Gaillard, T. Terre, J. Papadakis, M. Taroudakis, E. Skarsoulis, and C. Millot, "Acoustic observations of heat content across the mediterranean sea," *Nature*, vol. 385, no. 6617, pp. 615–617, Feb. 1997.

[13] Z. Zhu, X. Zhu, X. Guo, X. Fan, and C. Zhang, "Assimilation of coastal acoustic tomography data using an unstructured triangular grid ocean model for water with complex coastlines and islands," *J. Geophys. Res. Oceans*, vol. 122, no. 9, pp. 7013–7030, Sep. 2017.

[14] X.-H. Zhu, A. Kaneko, Q. Wu, C. Zhang, N. Taniguchi, and N. Gohda, "Mapping tidal current structures in zhitouyang bay, China, using coastal acoustic tomography," *IEEE J. Ocean. Eng.*, vol. 38, no. 2, pp. 285–296, Apr. 2013.

[15] Z. Zhao, Y. Zhang, W. Yang, and D. Chen, "High frequency ocean acoustic tomography observation at coastal estuary areas," in *Proc. AIP ConF*, Beijing, China, 2012, pp. 360–367.

[16] X. Yu, X. Zhuang, Y. Li, and Y. Zhang, "Real-time observation of range-averaged temperature by high-frequency underwater acoustic thermometry," *IEEE Access*, vol. 7, pp. 17975–17980, 2019.

[17] F. Syamsudin, N. Taniguchi, C. Zhang, A. D. Hanifa, G. Li, M. Chen, H. Mutsuda, Z. Zhu, X. Zhu, T. Nagai, and A. Kaneko, "Observing internal solitary waves in the lombok strait by coastal acoustic tomography," *Geophys. Res. Lett.*, vol. 46, nos. 17–18, pp. 10475–10483, Sep. 2019.

[18] M. Geawhari, L. Huff, N. Mhammdi, A. Trakadas, and A. Ammar, "Spatial-temporal distribution of salinity and temperature in the Oued Loukkos estuary, Morocco: Using vertical salinity gradient for estuary classification," *SpringerPlus*, vol. 3, no. 1, p. 643, 2014.

[19] J.-H. Park and A. Kaneko, "Assimilation of coastal acoustic tomography data into a barotropic ocean model," *Geophys. Res. Lett.*, vol. 27, no. 20, pp. 3373–3376, Oct. 2000.

[20] X. Yu and Y. Zhang, "Ray chaos in an architectural acoustic semi-stadium system," *Chaos: Interdiscipl. J. Nonlinear Sci.*, vol. 23, no. 1, Mar. 2013, Art. no. 013107.

[21] V. A. Del Grosso, "New equation for the speed of sound in natural waters (with comparisons to other equations)," *J. Acoust. Soc. Amer.*, vol. 56, no. 4, pp. 1084–1091, Oct. 1974.

[22] K. M. Jeffries, R. E. Connon, B. E. Davis, L. M. Komoroske, M. T. Britton, T. Sommer, A. E. Todgham, and N. A. Fangue, "Effects of high temperatures on threatened estuarine fishes during periods of extreme drought," *J. Exp. Biol.*, vol. 219, no. 11, pp. 1705–1716, Jun. 2016.

XIAOJIAN YU received the master's degree in landscape architecture from the University of Wisconsin-Madison, USA. She is currently an Associate Professor with the School of Biological Science and Biotechnology, Minnan Normal University. Her research interests include underwater acoustic tomography, smart city sensing, urban planning and theory, 3-D model, and city spatial analysis-based on complexity theory.

SONG LIN received the B.S. degree in marine physics from Xiamen University, Xiamen, China, in 2017, and the M.S. degree from the College of Ocean and Earth Science, Xiamen University, in 2020.

Since 2017, he has been a Research Assistant with the Key Laboratory of Underwater Acoustic Communication and Marine Information Technology, Ministry of Education. His research interest includes monitoring water velocity and temperature by using coastal acoustic tomography and underwater acoustic communication.

XIONGYE HONG is currently the Director of the Fujian Coastal Sea Environmental Monitoring Station, Putian, China. His research interests include hydrological monitoring, and environment monitoring in Minjiang Estuary and the coastal area of Putian.

HONGHUI HUANG is currently the Director of the Guangdong Provincial Key Laboratory of Fishery Ecology and Environment, South China Sea Fisheries Research Institute, Chinese Academy of Fishery Sciences, China. He has engaged in scientific research at the Southern Marine Science and Engineering Guangdong Laboratory (Guangzhou). His research interest includes ecological environmental monitoring and management in Daya Bay seawater.